Journal of Materials Chemistry A

Accepted Manuscript

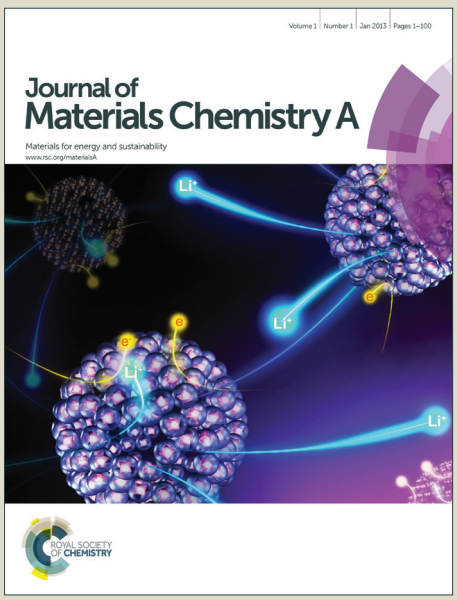

ROYAL SOCIETY OF CHEMISTRY

www.rsc.org/materialsA

Journal of Materials Chemistry A

Dynamic Article Links ►

Cite this: DOI: 10.1039/c0xx00000x

www.rsc.org/xxxxxx

ARTICLE TYPE

Effective synergistic effect of Al2O3 and SiC microparticles on the growth of carbon nanotubes and its application in high dielectric permittivity polymer composites

Anthony B. Dichiara,[a] Jinkai Yuan,[a] Shenghong Yao,[b] Alain Sylvestre, [b] Laurent Zimmer,[b] Jinbo Bai[a]*

Received (in XXX, XXX) Xth XXXXXXXXX 20XX, Accepted Xth XXXXXXXXX 20XX
DOI: 10.1039/b000000x

Owing to their excellent intrinsic properties, carbon nanotubes (CNTs) have been widely used to reinforce polymer composites. However, the CNT aggregation, the poor CNT/matrix nanoscale interface and the increased viscosity are perplexing issues limiting the applications of CNTs in polymer composites. A potential solution to achieve high dispersion states relies upon the concept of micro/nanoscale structures. Previous studies have reported a new generation of composites based on the hybridization of CNTs with ceramic microparticles, providing outstanding properties when used as fillers in polymer composites. Nevertheless, opportunities still exist to improve the performances of these composites further by mixing different types of CNT/ceramic hybrids in properly adjusted proportions. This work focuses on the growth of CNTs on different mixtures of alumina microspheres and silicon carbide microplatelets by floating-catalyst chemical vapor deposition (CVD). Not only the polyvinylidene fluoride composites prepared with the as-synthesized hybrid mixtures exhibit significant improvement of the dielectric properties than those reinforced with either component alone, but also the CVD process yields abnormally high CNT mass yield when the two types of ceramic particles were simultaneously used as substrate for the growth. The underlying mechanisms regarding both the CNT growth and the dielectric behaviour of the polymer composites were thoroughly investigated and discussed.

Introduction

The excellent mechanical[1] and electrical[2] properties of carbon nanotubes (CNTs) have spurred tremendous attention for years in the field of functional composites. For instance, nanotubes have been widely used to prepare high-dielectric-performance polymer composites,[3,4] which have attracted great interest due to their appealing applications in electromechanical actuators,[5] artificial muscle,[6] and capacitors for power energy storage.[7] The dielectric properties of these materials are proved to be strongly dependent on the underlying microcapacitor network of CNTs well below the percolation threshold.[8] The percolation, in general, is attributed to the formation of an infinite network of conductive fillers by interconnection in the polymer matrix.[9,10] Hence, the dielectric properties largely depend on the morphology and dispersion state of the conductive fillers. However, the CNT aggregation due to π–π interactions along their length axis and the nanoscale interface between the CNTs and the matrix strongly hinder the fabrication of high performance dielectric composites, usually inducing low dielectric permittivity, high leakage current, large dielectric loss and low breakdown strength, thus limiting practical applications.[11,12] While great efforts have been made to improve the dispersion of CNTs by the functionalization of various organic groups,[8,13] such methods mostly result in the deterioration of the CNT electrical properties.

Micro/nanoscale hybrid architectures combining CNTs with microsized reinforcements have proven high potential in composite applications.[14] The materials reinforced with low fractions of these CNT-based hybrids exhibit better properties than composites reinforced with either component alone. For instance, by growing CNTs on graphene nanoplatelets, it has been recently demonstrated that the interfacial strength between the fillers and the matrix could be greatly improved, because uniform dispersion of the fillers into the polymer matrix was achieved.[15,16] Additionally, when a small amount of CNT-based hybrids is incorporated into an insulated polymer matrix, the readily oriented CNTs on the micro ceramic particles give rise to a network of microcapacitors, thus improving the dielectric properties of the composite while maintaining the good insulation state of the polymer matrix.[17]

The present work describes the simultaneous growth of aligned multiwall CNTs (MWCNTs) on both alumina micro-spheres (μ-Al_2O_3) and silicon carbide micro-platelets (μ-SiC) by a floating-catalyst chemical vapor deposition (CVD) method, which has been extensively used to mass-produce CNT arrays on various substrates by decomposing a ferrocene-xylene mixture at relatively low temperature in a quartz tube reactor.[18] Mixing these ceramic microparticles together surprisingly revealed a synergistic effect on the CNT synthesis, significantly improving the mass yield, which was attributed to the increase of the CNT areal density, length and diameter in different proportions. Furthermore, aligned CNT layer grown on the surface of SiC or Al_2O_3 microparticles have already been used as individual reinforcements in multifunctional polymer composites, showing significant enhancements of the thermal,[19] mechanical[20] and electrical properties.[21] But, combining μ-SiC/CNT hybrids with

μ-Al_2O_3/CNT hybrids may create some new and exciting possibilities for their application in the fields of structural materials and electronic devices. Herein, we demonstrate that such mixture show significant synergistic effect on improving the dielectric properties of polyvinylidene fluoride (PVDF) composite while preserving the good insulating nature of the polymer matrix. The resultant high-permittivity composites can find potential applications in capacitors for power energy storage.

Experimental

CNT hybridization with ceramic micro-particles by CVD

The synthesis of the hybrids was carried out by a catalytic CVD process under atmospheric pressure. A 200 mm long quartz plate supporting the ceramic micro-particles (*i.e.* μ-Al_2O_3, size ranging in 1–5 μm, Performance Ceramics Company, and μ-SiC, size ranging in 1-5 μm, Marion Technologies) was put at the center of a quartz tube (45 mm in diameter and 1200 mm in length) which was then placed in a horizontal electrical resistance furnace (Carbolite HZS). Mixtures of μ-Al_2O_3 and μ-SiC were combined with various mass fractions and dispersed by a sieve agitator onto the center of the quartz plate, forming a small section of 25 mm^2 ± 5 mm^2. The total mass of the mixture was kept constant (0.05 g) and the different SiC/Al_2O_3 ratios used in this study are listed in **Table 1**. For consistency purposes, triplicate samples were prepared at each proportion. The reactor was heated up to 575°C under a mixture of argon (Ar – 99.8% purity – full scale: 10 L/min – 70 vol.%) and hydrogen (H_2 – 99.9% purity – full scale: 5 L/min – 30 vol.%). After 10 min for the system stabilization, a ferrocene/xylene solution concentrated at 0.05 g/mL was fed at 0.2 mL/min along with acetylene at 0.04 L/min (C_2H_2 – 99.6% purity – full scale: 1 L/min). The injection temperature of the ferrocene/xylene solution was set to 250°C for all experiments. The gas flows were controlled by thermal electronic mass flowmeters (Bronkhorst) while the liquid injection was adjusted by a mechanical syringe system fitted with a liquid flow meter (Razel Science, R99-E). The CNT growth on the ceramic particles lasted for 10 minutes before the furnace was cooled down to room temperature under 1 L/min of argon.

Table 1. The mass of each component in the hybrid/PVDF composites

Exp.	SiC/Al_2O_3 (wt.%)	Ceramic (g)	Hybrids (g)	CNTs (g)	PVDF (g)	Hybrid content (wt.%)
1	100/0	0.05	0.080	0.030	5.00	1.57
		0.4	0.630	0.230	-	-
2	70/30	0.05	0.130	0.080	5.00	2.53
3	50/50	0.05	0.185	0.135	5.00	3.57
4	30/70	0.05	0.140	0.090	5.00	2.72
5	0/100	0.05	0.105	0.055	5.00	2.06
		0.4	0.820	0.420	-	-

Preparation of the polymer composites

To prepare the composites, the as-synthesized hybrids were directly incorporated into the semi-crystalline polymer PVDF matrix (Kynar 721, Arkema Group) using a solution cast process followed by an extrusion method. The former aimed at the total penetration of PVDF solution into the aligned CNTs, while the latter ensured the uniform dispersion of the CNT hybrids throughout the composites. Briefly, the hybrids and the PVDF powder were first dispersed in the solvent N,N-dimethylformamide (DMF) by magnetic stirring overnight. All the composites were prepared with the same PVDF content (5 g). The mixed solution was then coated on a glass substrate and was thermally treated at 150°C for 2 hours. Afterwards, the as-prepared films were mixed in a co-rotating, conical, twin-screw micro-compounder (Micro 5 cm^3 Twin Screw Compounder, DSM) for 10 min at 200°C and at a mixing speed of 20 rpm under Ar atmosphere. Finally, 1.5 mm-thick slabs were prepared by injection molding (Micro 5 cm^3 Injection Molder, DSM) using a press at 1.6 MPa for 1 min at 60°C. By combining the solution cast and extrusion method, the CNT hybrids could be uniformly dispersed in PVDF matrix. Moreover the aligned CNTs were always well attached on the ceramic particles during the process. The morphologies of hybrids and their good dispersion state in the composites have been well confirmed in our previous work.[16-17, 20-21]

Characterization

Thermogravimetric (TG, Netzsch, STA 449 F3 Jupiter) analysis was used to determined the CNT mass after CVD synthesis. The as-grown hybrids were characterized by scanning electron microscopy (SEM, LEO Gemini 1530), transmission electron microscopy (TEM, JEOL 1200 EX) and high resolution electron microscopy (HRTEM, Philips CM20-UT).

The dielectric properties of the as-prepared composites were examined as a function of frequency using an impedance analyzer (Novocontrol BDS 20). Before measurement, silver paste was applied on the sample surfaces. The sample is then considered as a plane capacitor with an electrode surface area *S* and thickness *d*, and described by a parallel resistor-capacitor equivalent circuit. The complex dielectric permittivity (ε^*), complex impedance (Z^*) are calculated as follows:

$$\varepsilon^* = \varepsilon' - i\varepsilon'' \quad (1)$$

$$Z^* = Z' + iZ'' \quad (2)$$

Where ε' and ε'' are the real and imaginary parts of the complex dielectric permittivity; Z' and Z'' represent the real and imaginary part of the complex impedance. Starting from the impedance data, ones can calculate:

$$\varepsilon' = \frac{1}{\omega C_0}\frac{-Z''}{Z'^2 + Z''^2} \quad (3)$$

$$\varepsilon'' = \frac{1}{\omega C_0}\frac{Z'}{Z'^2 + Z''^2} \quad (4)$$

$$\sigma' = \omega \varepsilon_0 \varepsilon'' \quad (5)$$

$$\tan\delta = \frac{\varepsilon''}{\varepsilon'} \quad (6)$$

Where $\omega = 2\pi f$ is the angular frequency, $C_0 = \varepsilon_0 \frac{S}{d}$ is the free space capacitance.

Results and discussion

Influence of the substrate on CNT growth

The CNT structure depends not only on the synthesis parameters but also on the substrate used for the growth. In all CVD synthesis detailed in this work, the CNT self-assembly was found to always occur on the ceramic micro-particles (*i.e.* no CNT growth was observed neither on the reactor wall nor on the quartz plate supporting the ceramic micro-particles), as already reported in our previous study.[18] Moreover, the surface area of the alumina micro-spheres (*i.e.* πd^2, approximated by a sphere with diameter d) is about 57% higher than that of the SiC micro-platelets (*i.e.* $2d^2$, approximated by a cuboid with base d), while the CNT mass was 83% larger on the former particles than on the latter ones, as listed in **Table 1**. Therefore, it means that Al_2O_3 micro-particles yield more efficient CNT growth than their SiC counterparts under the exact same CVD parameters. Larger CNT yields were also observed on Al_2O_3.[22] This unambiguously demonstrates the influence of the substrate's nature on the CNT synthesis. Furthermore, the mass of CNTs synthesized on Al_2O_3 (exp. 5) was found to be 83% higher than that on SiC (exp. 1) independently of the mass of the ceramic micro-particles introduced in the CVD reactor, as detailed in **Table 1**. This indicates that under similar conditions, the mass of CNT is proportional to the total surface area of Al_2O_3 micro-spheres and SiC micro-platelets separately, as long as the mass of the ceramic micro-particles introduced in the CVD reactor does not change the experimental conditions (*e.g.* diffusion of the precursors in the reactor, temperature profile...). This also shows the effect of the substrate's morphology on the CNT growth.

Under similar CVD conditions, the relatively high H_2 ratio was reported to significantly accelerate the ferrocene decomposition,[18,23] leading to large quantities of iron nanoparticles in the atmosphere which are deposited instantly on the substrate's surface. It has been recognized that these small catalyst particles are in closer interaction with their environment due to their large surface/volume ratio. Therefore, they are more sensitive to support effects. For instance, gold nanoclusters were catalytically active when deposited on Fe_3O_4, FeO or TiO_2 but inactive when deposited on Al_2O_3 under similar conditions.[24-26] In general, two aspects should be considered when dealing with the interactions of catalyst nanoparticles with their supports: (i) the electronic interaction corresponding to the charge redistribution at the catalyst-support interface and (ii) the chemical interaction corresponding to atom diffusion at the catalyst–support interface. In the case of insulating oxide supports such as Al_2O_3, local charge redistribution occurs within the first few atomic layers at the catalyst-support interface, driven by the difference of electronegativities between the catalyst nanoparticles and the support.[27] Such electronic interaction may enhance the catalytic properties of the nanoparticles, thus inducing higher CNT yield. However, in the case of SiC, the physical encapsulation of the catalyst particles by a thin layer of carbon on the carbon-rich facets might decrease the number of active catalyst particles for CNT growth,[28] while the silicon-rich facets may react with the iron catalysts to form silicon-iron compounds (*e.g.* $FeSi_2$, Fe_2SiO_4) which are not favorable for the growth of CNTs.[29]

Evidence for a synergistic effect by mixing Al_2O_3 with SiC micro-particles

As previously detailed, the CNT mass is significantly affected by both the nature and the morphology of the substrate used for the synthesis. Since Al_2O_3 leads to higher CNT yields than SiC independently of the mass of ceramic micro-particles introduced in the CVD reactor, intermediate CNT masses would be expected when mixing Al_2O_3 and SiC together during the same CVD synthesis. Three CNT growths were performed using different SiC/Al_2O_3 proportions but same total mass, as listed in **Table 1**. TGA showed that each sample has a small content of amorphous carbon of 3 wt.% and a relatively high oxidation stability of about 580°C. **Figure 1** displays the evolution of the CNT mass yield determined by TGA as a function of the SiC/Al_2O_3 ratio.

Unlike previous expectations, the as-grown CNT masses reported on the mixed ceramic micro-particles are surprisingly much higher than that measured on Al_2O_3 micro-spheres. The CNT masses on the 70:30, 50:50 and 30:70 mixtures are indeed 45, 145 and 64 % higher than that on the individual Al_2O_3 micro-spheres, and about 167, 350 and 300% higher than that on the individual SiC micro-platelets, respectively. In addition, the CNT mass yield reaches a maximum of 73 wt.% when the mixture composing the support for the CNT growth is formed by an equal amount of Al_2O_3 and SiC. As a comparison, Singh et al[30] reported a CNT mass yield of 66 wt.% on ball milled silica using a solution of ferrocene/toluene at 700°C for 90 min. This unambiguously revealed a synergistic effect on the CNT

growth by mixing these two types of ceramic micro-particles.

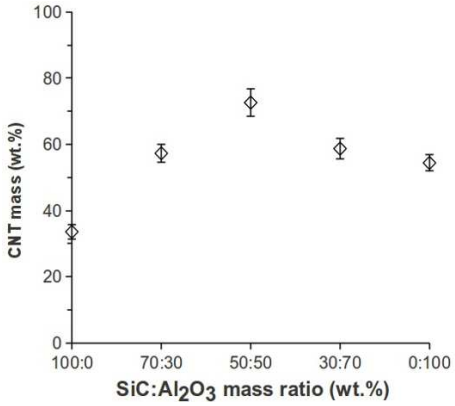

Figure 1. Evolution of the CNT mass yield as a function of the SiC/Al_2O_3 ratio.

Influence of the synergistic effect on the CNT structure

Electron microscopy observations of the samples listed in **Table 1** show that in each case vertically aligned multi-walled CNTs were grown perpendicular to their support (*i.e.* μ-SiC and μ-Al_2O_3), as depicted in **Figure 2**. This is consistent with previous studies reporting the growth of CNTs on ceramic particles under similar CVD conditions.[31-33] In all samples, the average CNT length was determined for each type of ceramic micro-particle by measuring the height of about fifty different CNT forests using SEM. **Figure 3a** presents the average CNT length on Al_2O_3 micro-spheres (♦) and on SiC micro-platelets (■) in each sample. It can be seen that the CNT length on Al_2O_3 micro-spheres gradually increases with the addition of SiC micro-platelets in the mixture. The average CNT length on Al_2O_3 rises up to 16.9, 17.5, 18.4 and 19.7 μm, when the amount of SiC in the mixture reaches 0, 30, 50 and 70 wt.%, respectively. Reversely, the CNT length on SiC reduced with the decrease of the SiC micro-platelets present in the mixture. The average CNT length on SiC was 21.8 to 15.5, 14.9 and 14.4 μm when the mass ratio of Al_2O_3 in the mixture was 0, 30, 50 and 70 wt.%, respectively. Hence, the opposite trends of the average CNT length observed when mixing the two types of ceramic micro-particles together cannot explain the increase of the CNT mass observed in **Figure 1**.

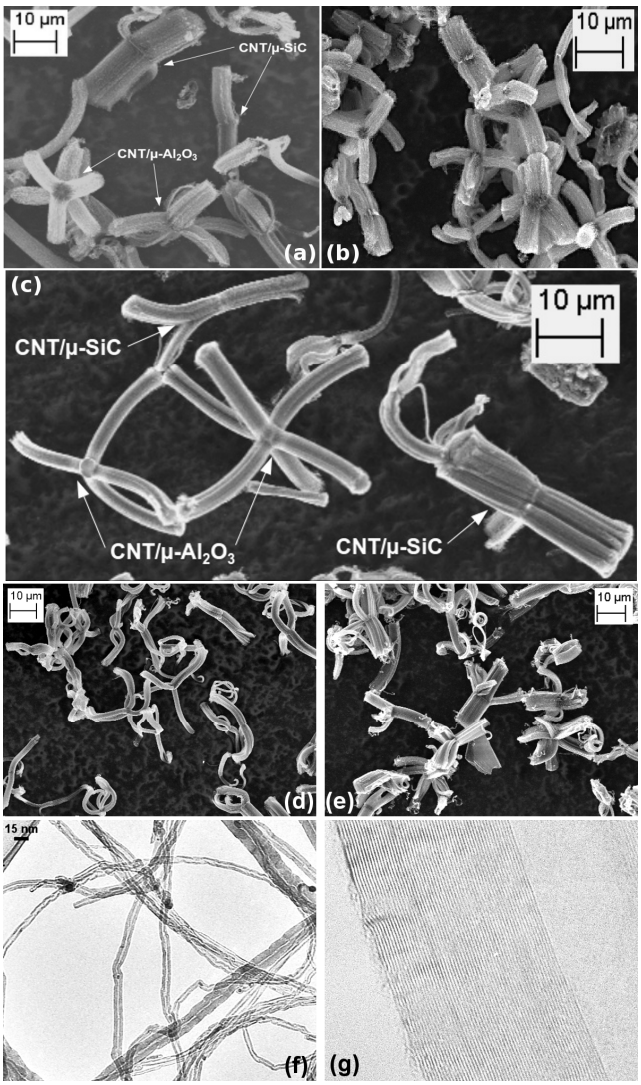

Figure 2. SEM images of the mixture samples referred to as exp. 2 (a), 3 (b) and 4 (c) in Table 1 and the individual samples from exp. 1 (d) and 5 (e). HRTEM images of typical as-grown MWCNTs (f-g).

Similarly, the CNT diameter in all samples and for each type of ceramic micro-particle was averaged over about fifty individual CNTs using TEM. **Figure 3b** shows the average CNT diameter on Al_2O_3 micro-spheres (diamonds) and on SiC micro-platelets (squares) in each sample. It was found that the CNT diameter on the SiC micro-platelets remained in the same range, while that on the Al_2O_3 micro-spheres increased with the addition of SiC in the mixture. The average CNT diameter on SiC was ranging between 12.78 and 13.17 nm, while that on Al_2O_3 gradually increases to 9.09, 9.95, 10.87 and 11.38 nm when the mass ratio of SiC contained in the mixture was set to 0, 30, 50 and 70 wt.%, respectively.

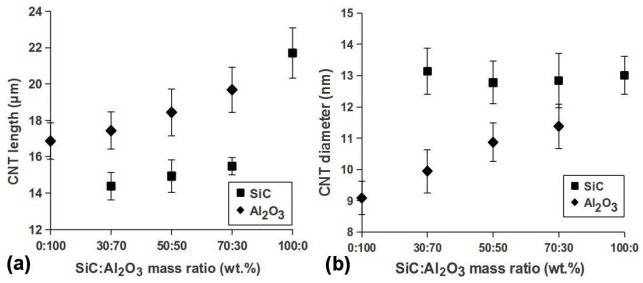

Figure 3. Evolution of the CNT length (a) and diameter (b) on each ceramic particle as a function of the SiC/Al_2O_3 mass ratio.

Using the relation proposed elsewhere,[34] the weight of a single MWCNT with an inner diameter of 9 nm and an outer diameter of 11.4 nm divided by that of a CNT, 9 nm in diameter, yields the mass gain when both substrates are mixed together. Since the evolution of the

CNT length on one substrate was found to be counter-balanced by that on the other support, the CNT length was supposed to be globally invariant. In addition, the aspect ratio of the CNTs is sufficiently high (>1000) to neglect the area of the section surfaces in comparison to that of the cylindrical surfaces, while the length of the C=C bonds in the CNT curved graphene sheets is supposed to be the same than in the planar sheet (*i.e.* $d_{c=c}$ = 0.1421 nm). Hence, a maximum of 76 wt.% increase of the total CNT mass can be deduced in the mixture yielding the largest CNT diameters.

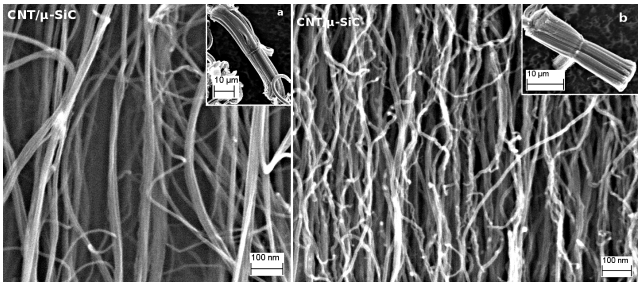

Figure 4. Representative electron microscopy images of the CNTs grown on SiC from sample 1 (a) and sample 3 (b). The bulk CNT density is obviously higher when the two ceramic particles are mixed together. Low magnification SEM images of the corresponding CNT/μ-SiC hybrids are shown in the insets.

This result is overestimated, as for the ease of calculation, every CNTs in the mixture were supposed to undergo the same diameter increase. Despite these observations, the increase of the CNT diameter is not sufficient to fully describe the evolution of the CNT mass depicted in **Figure 1**, which ultimately depends on the CNT areal density. Whereas it is almost impossible to quantify by SEM, obvious changes in the CNT areal density can be observed when the two types of ceramic particles are mixed together compared with the CNT growth on a single type of substrate, as depicted in **Figure 4**. Chiodarelli et al.[35] proposed an empirical law correlating the average number of walls to the average CNT diameter in a population of MWCNTs grown by CVD. This relationship arising from statistical analysis of data originated from independent sources, including CNTs grown under various conditions with a variety of CVD tools, it can be considered as general validity. The weight of the sample determined by TGA corresponding to the amount of carbon atoms present in the as-grown CNTs, the equation suggested by Chiodarelli et al.[35] can be thus used to estimate the average number of MWCNTs from weight measurements. Such approach was already proposed by Zhong et al.[36] for single wall CNTs. Therefore, the number of CNTs produced (N_{CNT}) can be modeled by the following equation,

$$N_C \approx 0.66\Omega_C\pi\left(\frac{l_{CNT}d_{CNT}^2}{10^{-9}}\right) \qquad (7)$$

where N_C corresponds to the amount of carbon atoms forming a MWCNT of diameter d and length l, m_C stands for the mass of a carbon atom ($m_C = 1.993 \cdot 10^{-26}$ kg) and m_{CNT} is the total mass of the as-produced CNTs: $N_{CNT} = m_{CNT} / (N_C \cdot m_C)$. Ω_C is the surface density of carbon atoms in CNT (*i.e.* $\Omega_C = 3.872.10^{19}$ m^{-2}). Given the average CNT lengths and diameters reported in **Figure 3**, the number of CNTs synthesized on the SiC micro-platelets, the Al_2O_3 micro-spheres and the mixture formed by an equal amount of each type of ceramic micro-particles is estimated to $5.1.10^{12}$, $2.5.10^{13}$, $3.39.10^{13}$, respectively. The amount of CNTs in the mixture is about 36 and 565% higher than that on Al_2O_3 and SiC alone. This is consistent with electron microscopy observations at higher magnification, revealing the increase of the CNT areal density on SiC in the mixture (**Figure 4**). Therefore, the CNT mass gain observed in **Figure 1** on the different mixtures arises from an increase of both CNT diameter (mostly on Al_2O_3) and CNT areal density (mainly on SiC).

The as-reported synergistic effect induced by the mixture of different ceramic particles during CVD synthesis of CNTs is quite surprising. We hypothesize that the ceramic mixture may contribute to the formation of chemical intermediate species leading to the growth of CNTs. The role of oxygen in supergrowth of CNTs[37] might suggest that oxygen in μ-Al_2O_3 could promote the synthesis of CNTs via the decomposition of SiC.[38,39] Although the catalytic reactivity of various oxide surfaces have been shown to dissociate H=H, C=H, C=C and C=O, bonds,[40,41] it is not not clear whether the observed phenomena is solely due to this dependency. It is also known that defects are usually responsible for many of the catalytic and chemical properties. For instance, defect sites in CVD synthesis of CNTs have previously been implicated in the observed graphitic anchoring and formation with the graphitic layers formed on the crystalline oxide particles shown to root at step sites.[42,43] Further studies will be required to unravel the growth mechanism related to this synergistic effect.

Applications in high permittivity dielectric polymer composites

To explore the application of the aforementioned synergistic effect in polymer composites, we prepared a series of PVDF composites by using hybrid mixture with different SiC/Al_2O_3 ratios. **Figure 5** shows the dielectric permittivity, AC conductivity and loss tangent at 100 Hz for different composites. The dielectric permittivity (**Figure 5a**) of the composite reinforced with μ-SiC hybrid alone is 24 at 100 Hz, which is about 2 times larger than that of pristine PVDF (10~13).[44] With the increase of the μ-Al_2O_3 mass ratio in the mixture, the dielectric permittivity of the composites increases accordingly and reaches the maximum (*i.e.* 346) at SiC/Al_2O_3=50:50. After that, the permittivity starts to decrease with increasing the μ-Al_2O_3 ratio further until reaching the lowest value (*i.e.* 19) in the composite reinforced by μ-Al_2O_3 hybrid alone. In the CNT-based hybrids/PVDF composites, the increase in the dielectric permittivity can be derived from the formation of microcapacitors as a result of readily aligned state of nanotubes on the microparticles.[17] In the case of

SiC/Al_2O_3=50:50, the highest CNT density on μ-SiC could form the largest number of microcapacitors inside composites. Moreover, the increased diameter and length of nanotube on μ-Al_2O_3 would make the readily formed microcapacitor more efficient. Both facts would afford a largest permittivity value. The AC conductivity exhibits almost the same trend as that of the dielectric permittivity, as depicted in **Figure 5b**. It should be emphasized that even the maximum conductivity is still very low (*i.e.* 2.7×10^{-7} $S.m^{-1}$) for dielectric applications, indicating a good insulating nature of the composite. This is further confirmed by the low loss values (*i.e.* <0.13) found for all the as-prepared dielectric composites, as shown in **Figure 5c**.

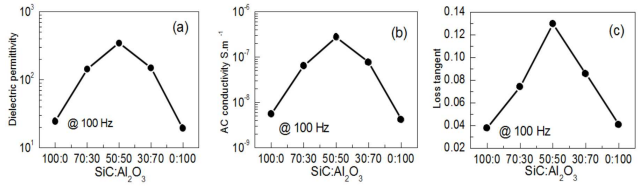

Figure 5. Evolution of the dielectric permittivity (a), the AC conductivity (b) and the loss tangent (c) as a function of the SiC/Al_2O_3 mass ratio in the polymer composites.

To better understand the dielectric behaviors of as-prepared composites. The frequency dependences of dielectric properties are plotted in **Figure 6**. The dielectric permittivity (**Figure 6a**) of composites with μ-SiC or μ-Al_2O_3 hybrids alone decreases slightly with frequency, which displays good frequency stability. This frequency independence arises from the microcapacitor structure nature that induces the increment in dielectric permittivity.[17,45] On the other hand, higher dielectric permittivities are observed over a broad frequency range in the composites with SiC/Al_2O_3=70:30 or 30:70. In these two cases, the increased mass yield of CNTs largely favors the formation of more effective microcapacitors meanwhile avoids the direct contact between neighboring hybrids. This point can be clearly verified by the frequency dependence of AC conductivity of composites shown in **Figure 6b**. It is noted that the composites with SiC/Al_2O_3=70:30 or 30:70 exhibit strong frequency dependence, showing a nearly linear increase with the frequency. This implies a good insulating nature of the composites, which is very desirable for applications in capacitors as dielectrics. Owing to the absence of the conductive path inside composites, the conductivity is dominated by the polarization effects and the electron motion of the PVDF matrix, which highly depends on the frequency. Consequently a frequency-dependent AC conductivity is exhibited. Moreover, the microcapacitors are also considered to contribute to the AC conductivity. Generally, the more microcapacitors formed inside composites, the more AC current passing through the capacitors. That is why higher conductivities are found at high mass content as in the case of composites SiC/Al_2O_3=70:30 or 30:70. Of particular note is that the dielectric permittivity of the composite with SiC/Al_2O_3=50:50 exhibits highest frequency dependence as compared with its counterparts. In this case, the tunneling between neighboring hybrids possibly occurs due to the increased nanotube length on μ-Al_2O_3 as well as the decreased inter-tube distance on μ-SiC. This largely favors the charge injection from the external electrodes so that a large number of charge carriers are accumulated at the CNT-polymer interfaces inside the microcapacitors.[46] This interfacial polarization, also known as the Maxwell-Wagner-Sillars effect, is responsible for the enhancement of dielectric permittivity observed at low frequency.[44] Furthermore, in the composite with SiC/Al_2O_3=50:50, the largest amount of CNTs (as shown in **Table 1**) gives rise to the highest interfacial areas, which could also significantly reinforce the Maxwell-Wagner-Sillars effect by providing polarization sites. The tunneling can also induce an increased AC conductivity, especially at low frequencies, which can be clearly seen in **Figure 6b**.

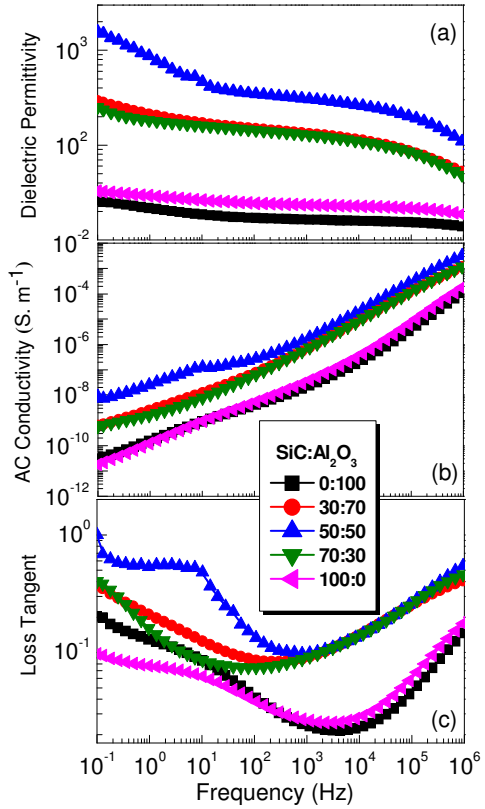

Figure 6. Frequency dependence of (a) the dielectric permittivity, (b) AC conductivity and (c) loss tangent of the CNT-based hybrids/PVDF composites with different SiC/Al_2O_3 mass ratios.

Figure 6c presents the loss tangent of the composites as a function of frequency. Generally, the dielectric loss consists of two parts: one is due to the Debye-type relaxation, and the other originates from the leakage current that results from the tunneling between neighboring conductive particles.[47] When there is no conductive path formed in the composites, as the case of composites with μ-SiC or μ-Al_2O_3 hybrids alone, the loss of composites exhibits the typical relaxations of PVDF matrix.[48] The attained much low loss (~0.09 at 100 Hz) is believed to come from the Debye-type relaxation in the polymer matrix. However, for the composites with hybrid mixtures, the loss tangent was increased, indicating that apart from the Debye-type relaxation in the polymer matrix, there is an additional factor that contributes to the loss. Considering the fact that the interactions between neighboring hybrids would possibly occur as more and longer nanotubes are yielded on the microparticles at SiC/Al_2O_3=50:50, the slight increase of loss from 0.09 to 0.13 at 100 Hz possibly originates from the leakage current across

the external electrodes as a result of the tunneling effect between CNT arrays of neighboring hybrids in the case of SiC/Al_2O_3=50:50 composite. Moreover, the dielectric loss tangent of each composite remains at a low value (< 0.13) in a wide frequency range from 10^1 to 10^6 Hz, which is much lower than other composites with similar loading of carbon nanomaterials (> 3 wt.%).[17] A low dielectric loss of the composites is of paramount importance for further applications in electric-energy-storage capacitors.

Conclusions

We have reported the simultaneous growth of aligned MWCNTs on both μ-Al_2O_3 and μ-SiC by a floating-catalyst CVD method. Mixing these ceramic micro-particles together surprisingly revealed a synergistic effect on the CNT synthesis, significantly improving the mass yield. A maximum CNT mass yield of 73 wt.% was achieved after 10 minutes at 575 °C when an equal amount of each ceramic μ-particle was used as the substrate, which is nearly twofold larger than the CNT growth on either component alone. The enhanced CNT yield on the mixture is attributed to the increase of the CNT areal density, length and diameter in different proportions on each type of ceramic μ-particle, possibly caused by an increasing amount of defects on their surface and/or the promotion effect of the chemical intermediate reactions. These micro/nanoscale hybrid structures were further employed to fabricate dielectric polymer composites by a solution-cast and extrusion method. The obtained composites exhibit not only a high dielectric permittivity but also maintain low dielectric loss over a wide frequency range, which is attributed to the largely formed microcapacitors composed of the aligned CNTs as electrodes and the insulating polymer matrix in between as dielectric. The good dispersion of the hybrids in the PVDF matrix also helps to suppress the leakage current by preventing the hybrids from contacting. Furthermore, the dielectric permittivity of the composites can be tuned by tailoring the content of μ-Al_2O_3/CNTs and μ-SiC/CNTs. Though further optimizations are still needed, the introduction of multiple types of CNT-based hybrids can endow the resulting composites with enhanced dielectric properties, providing great potential for power energy storage applications.

Acknowledgements

The authors thank Marion Technologies for supplying the μ-SiC particles. J.K. Yuan acknowledges the financial support of China Scholarship Council. The authors are also grateful to F. Garnier and P. Haghi-Ashtiani for their help with SEM and TEM observations, respectively.

Notes and references

[a] *Lab. MSSMat, CNRS UMR8579, École Centrale Paris, Grande Voie des Vignes, 92290 Châtenay-Malabry, France. Tel: (0033)1 41 13 13 16; E-mail: jinbo.bai@ecp.fr*
[b] *Lab. G2E, CNRS UMR5269, Joseph Fourier University, 25 rue des Martyrs, 38042 Grenoble, France*
[c] *Lab. EM2C, CNRS UPR288, École Centrale Paris, Grande Voie des Vignes, 92290 Châtenay-Malabry, France*

1 A. Yu, P. Ramesh, X. Sun, E. Bekyarova, M. E. Itkis, *Adv. Mater.* 2008, **20**, 4740.
2 A. G. Nasibulin, P. V. Pikhitsa, H. Jiang, D. P. Brown, A. V. Krasheninnikov, A. S. Anisimov, et al. *Nat. Nanotechnol.* 2007, **2**, 156.
3 S. H. Yao, J. K. Yuan, T. Zhou, Z. M. Dang, J. Bai. *J. Phys. Chem. C.*, 2011, **115**, 20011.
4 C. Wu, X. Huang, X. Wu, L. Xie, K. Yang, P. Jiang, *Nanoscale*, 2013, **5**, 3847.
5 C. Li, E. T. Thostenson, T. W. Chou. *Comp. Sci. Technol.*, 2008, **68**, 1227.
6 S. Zhang, N. Zhang, C. Huang, K. Ren, and Q. M. Zhang, *Adv. Mater.*, 2005, **17**, 1897.
7 Z. M. Dang, J. K. Yuan, S. H. Yao, R. J. Liao, *Adv. Mater.* 2013, **25,** 6334–6365.
8 Z. M. Dang, L. Wang, Y. Yin, Q. Zhang, Q. Q. Lei, *Adv. Mater.*, 2007, **19**, 852.
9 A. V. Kyrylyuk, M. C. Hermant, T. Schilling, B. Klumperman, C. E. Koning, P. van der Schoot, *Nat. Nanotechnol.*, 2011, **6**, 364.
10 S. De, P. J. King, P. E. Lyons, U. Khan, J. N. Coleman, *ACS Nano*, 2010, **4**, 7064.
11 E. T. Thostenson, Z. Ren, T.-W. Chou, *Comp. Sci. Technol.*, 2001, **61**, 1899.
12 J.-H. Du, J. Bai, H.-M. Cheng, *eXPRESS Polymer Lett.*, 2007, **1**, 253.
13 N. G. Sahoo, S. Rana, J. W. Cho, L. Li, S. H. Chan, *Prog. Polym. Sci.*, 2010, **35**, 837.
14 L. Ci, J. Bai, *Adv. Mater.* 2004, **16**, 2021.
15 W. Li, A. Dichiara, J. Bai, *Comp. Sci. Technol.*, 2013, **74**, 221.
16 A. Dichiara, J. K. Yuan, S. H. Yao, A. Sylvestre, J. Bai, *J. Nanosci. Nanotechnol.* 2012, **12**, 6935.
17 J. K. Yuan, W. L. Li, S. H. Yao, Y. Q. Lin, A. Sylvestre, J. Bai, *Appl. Phys. Lett.* 2011, **98**, 032901.
18 A. Dichiara, J. Bai, *Dia. & Rel. Mater.* 2012, **29**, 52.
19 M. Bozlar, D. He, J. Bai, Y. Chalopin, N. Mingo, S. Volz, *Adv. Mater.* 2010, **22**, 1654.
20 W. Li, J. K. Yuan, A. Dichiara, Y. Lin, J. Bai, J. *Carbon* 2012, **50**, 4298.
21 W. Li, J. K. Yuan, Y. Lin, S. Yao, Z. Ren, H. Wang, M. Wang , J. Bai, *Carbon*, 2013, **51**, 355.
22 R. Seidel, G. S. Duesberg, E. Unger, A. P. Graham, M. Liebau, F. Kreupl, *J. Phys. Chem. B*, 2004, **108**, 1888.
23 K. Kuwana, K. Saito, *Proc. Combust. Inst.*, 2007, **31**, 1857.
24 D. C. Meier, D. W. Goodman, J. Am. Chem. Soc., 2004, **126,** 1892.
25 M. Haruta, N.Yamada, T. Kobayashi, S. Iijima, *J. Catal.* 1989, **115**, 301.
26 C.R. Henry, *Surf. Sci. Rep.* 1998, **31**, 231.
27 Q. Fu, T. Wagner, *Surf. Sci. Rep.* 2007, **62**, 431.
28 Z. Liu, L. Ci, V. Srot, N. Y. Jin-Phillipp, P. A. van Aken, M. Rühle, J. C. Yang, *Appl. Phys. Lett.*, 2008, **93**, 233113.
29 M. Kusunoki, T. Suzuki, T. Hirayama, N. Shibata, K. Kaneko, *Appl. Phys. Lett.,* 2000, **7**, 531.
30 C. Singh, M. S. P. Shaffer, K. K. K. Koziol, I. A. Kinloch, A. H. Windle, *Chem. Phys. Lett.,* 2003, **72**, 860.
31 D. He, M. Bozlar, M. Genestoux, J. Bai, *Carbon,* 2010, **48**, 1159.

32 Q. Zhang, J.-Q. Huang, M.-Q. Zhao, W.-Z. Qian, Y. Wang, F. Wei, *Carbon*, 2008, **46**, 1152.
33 D. He, H. Li, W. Li, P. Haghi-Ashtiani, P. Lejay, J. Bai, *Carbon*, 2011, **49**, 2273.
34 Ch. Laurent, E. Flahaut, A. Peigney, *Carbon,* 2010, **48**, 2994.
35 N. Chiodarelli, O. Richard, H. Bender, M. Heyns, S. De Gendt, G. Groeseneken, P. M. Vereecken, Carbon, 2012, **50**, 1748.
36 G. F. Zhong, T. Iwasaki, H. Kawarada, *Carbon,* 2006, **44**, 2009.
37 T. Yamada, A. Maigne, M. Yudasaka, K. Mizuno, D. Futaba, M. Yumura, S. Iijima, K. Hata, *Nano Lett.*, 2008, **8**, 4288.
38 M. Kusunoki, T. Suzuki, K. Kaneko, M. Ito, Philos. Mag. Lett. 1999, **79**, 153.
39 M. Kusunoki, T. Suzuki, T. Hirayama, N. Shibata, K. Kaneko, *Appl. Phys. Lett.*, 2000, **77**, 531.
40 D. S. Jackson, S. J. S. Hargreaves, Metal Oxide Catalysis, Wiley-VCH: Weinheim, Germany, 2009
41 G. A. Somorjai, *Chem. Eng. News*, 2008, **86**, 15.
42 M. H. Rummeli, C. Kramberger, A. Gruneis, A. Ayala, T. Gemming, B. Buchner, T. Pichler, *Chem. Mater.* 2007, **19**, 4105.
43 M. H. Rummeli, F. Schaffel, A. Bachmatiuk, D. Adebimpe, G. Trotter, F. Borrnert, A. Scott, E. Coric, M. Sparing, B. Rellinghaus, P. G. McCormick, G. Cuniberti, M. Knupfer, L. Schultz, B. Buchner, *ACS Nano*, 2010, **4**, 1146.
44 J. K. Yuan, S. H. Yao, A. Sylvestre, J. Bai, *J. Phys. Chem. C*., 2012, **116**, 2051.
45 Q. Chen, P. Y. Du, L. Jin, W. J. Weng, G. R. Han, *Appl. Phys. Lett.*, 2007, **91**, 3.
46 M. Wong, M. Paramsothy, X. J. Xu, Y. Ren, S. Li, K. Liao, *Polymer*, 2003, **44**, 7757.
47 C. W. Nan, Y. Shen, J. Ma, *Annual Rev. Mater. Res.*, 2010, **40**, 131.
48 J. K. Yuan, S. H. Yao, Z.-M. Dang, A. Sylvestre, M. Genestoux, J. Bai, *J. Phys. Chem. C.*, 2011, **115**, 5515.

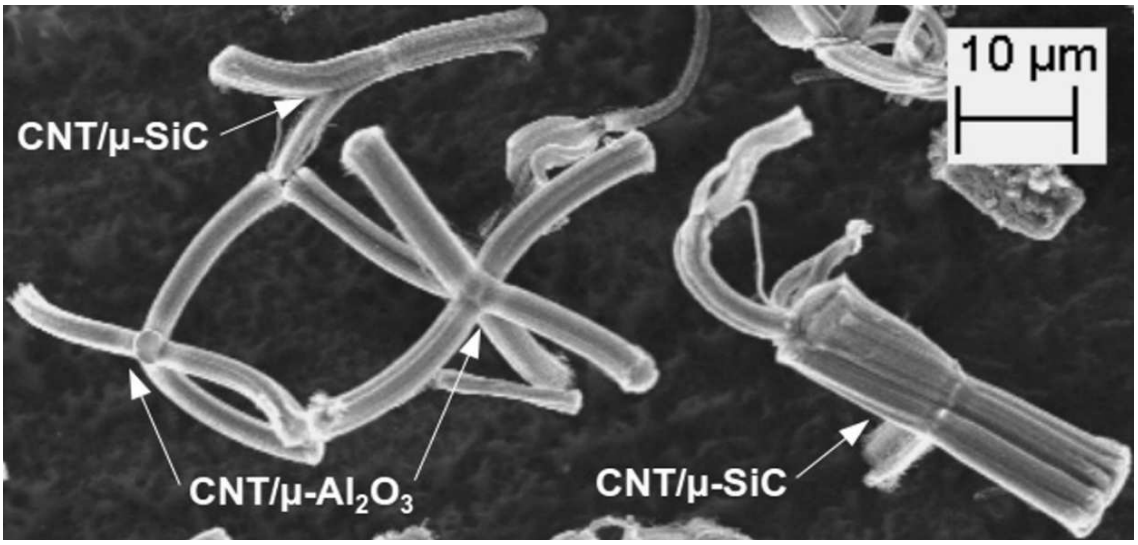

Opportunities exist to improve the performances of polymer composites by mixing different types of carbon nanotube/ceramic micro-particle hybrids in properly adjusted proportions. Not only the composites prepared with various types of hybrids exhibit much higher dielectric properties than those reinforced with either component alone, but also the synthesis process results in abnormally high CNT mass yields.